Research Square

Preprints are preliminary reports that have not undergone peer review.
They should not be considered conclusive, used to inform clinical practice,
or referenced by the media as validated information.

Uncertainty Aware Probabilistic Modelling of Terrestrial Free Space Optical Links under South African Continental Fog

Phatle Solly Maswikaneng

maswikanengps@tut.ac.za

Tshwane University of Technology

Article

Keywords: free-space optical communication, continental fog, meteorological optical range, probabilistic attenuation, South Africa, uncertainty quantification

Posted Date: November 3rd, 2026

DOI: https://doi.org/10.21203/rs.3.rs-11288809/v1

License: This work is licensed under a Creative Commons Attribution 4.0 International License.
Read Full License

Additional Declarations: No competing interests reported.

Uncertainty Aware Probabilistic Modelling of Terrestrial Free Space Optical Links under South African Continental Fog

Phatle Solly Maswikaneng

Department of Information Technology, Tshwane University of Technology, Pretoria, South Africa

Corresponding author: maswikanengps@tut.ac.za

Abstract

Fog is the dominant availability constraint for many terrestrial free-space optical (FSO) links, yet South African planning studies often report mean losses without distinguishing among visibility conventions, path lengths, and tail risk. This paper develops an uncertainty-aware, reproducible framework using peer-reviewed summaries derived from South African Weather Service observations rather than claiming access to station-level records. The model follows Recommendation ITU-R P.1814-1 (2025): meteorological optical range is converted to wavelength-dependent attenuation, propagated through Beer-Lambert loss, and transformed into fade-margin and outage quantities. A numerical audit of a published seven-location, three-wavelength South African table provides independent verification of implementation. The reported values are reproduced by a 0.23 km path calculation with a fixed wavelength exponent q=1.3, giving R^2=0.999998, root-mean-square error 2.52×10^{-4} dB, and mean absolute percentage error 0.133%. Back-calculated effective path lengths have a mean of 0.22997 km and a standard deviation of 0.00049 km. Accordingly, those values should be interpreted as approximately 230 m path losses rather than specific attenuation in dB/km. Scenario analysis then quantifies uncertainty from visibility error, wavelength exponent selection, and link length. Dense fog below 0.5 km suppresses the wavelength advantage in the ITU model; reducing span length therefore dominates wavelength selection for catastrophic events. Published exceedance probabilities above 80 dB/km imply approximately 33.3, 22.8, and 10.5 h $year^{-1}$ of severe exposure in Mbombela, Cape Town, and Polokwane, respectively, when treated as climatological frequencies. The framework provides auditable equations and conservative design rules while identifying that station-level validation is still required before site acceptance.

Keywords: free-space optical communication; continental fog; meteorological optical range; probabilistic attenuation; South Africa; uncertainty quantification

1 Introduction

Terrestrial FSO communication provides fibre-like capacity without a physical cable, but its optical beam is exposed to scattering, absorption, turbulence, pointing error and background radiation. Fog is especially damaging because its droplets are comparable in size to those in the visible and near-infrared wavelengths. Recent experimental and modelling results show that dense fog at 0.05 km visibility can produce approximately 339 dB km^{-1} of attenuation, demonstrating that relatively small changes in visibility or link length can determine whether an FSO link remains operational (Tarimo et al. 2026).

South Africa contains coastal, highveld, subtropical and arid microclimates. Kolawole et al. (2022) analysed SAWS-derived visibility observations for nine cities from January 2010 to June 2018 and reported strong spatial variation in fog frequency and attenuation exceedance. Maswikaneng et al. (2022) reported three-year mean visibility and wavelength-specific losses for seven locations. These studies establish the local relevance of visibility-based FSO planning while highlighting three important methodological and design considerations: mean visibility alone cannot determine outage probability; a

reported attenuation value cannot be interpreted accurately without a specified link distance; and a fitted statistical distribution cannot be independently validated without access to station-level observations.

This study addresses those issues as a physics-informed secondary analysis. Its original contributions are: (1) a convention-explicit formulation aligned with the current ITU-R P.1814-1 recommendation; (2) a numerical reproduction audit of the South African seven-location benchmark; (3) model-form and visibility uncertainty envelopes; (4) analytical conversion of fade margin to critical visibility and maximum span; and (5) a validation protocol that distinguishes implementation verification from empirical validation. This study is based on previously published SAWS-derived summaries; the underlying station-level records were not accessed, and no new site-specific probability distribution was fitted.

2 Data Sources and Methodological Framework

2.1 South African data

The first evidence stream is the visibility analysis of Kolawole et al. (2022), based on nine South African cities and observations at 08:00, 14:00 and 20:00 over 8.5 years. It supplies fog-frequency statements and selected attenuation exceedance probabilities. The second stream is the 2016-2018 summary of Maswikaneng et al. (2022), which provides mean visibility and reported loss at 650, 850 and 1550 nm for seven locations. These are published aggregates, not a substitute for the underlying SAWS time series.

Table 1. Data sources, analytical applications, and validation scope

Evidence item	Coverage	Use in this study	Validation status
Visibility distributions	9 cities; Jan 2010-Jun 2018; 3 observations daily	Published fog and exceedance probabilities	External benchmark only
Mean visibility and loss	7 locations; 2016-2018; 3 wavelengths	Equation and path-length reproduction audit	Numerical verification
Raw station observations	Not supplied with the present study	Required for refitting and hold-out tests	Future empirical validation
ITU-R P.1814-1	Terrestrial FSO paths; 0.4-1.55 μm model	Current physical and statistical framework	Normative model basis

2.2 Reproducible workflow

Figure 1 separates sourced quantities from derived quantities. Published visibility and probability summaries are entered into the calculation unchanged. The present study contributes transformations, diagnostics, uncertainty bounds and design implications. This separation prevents a secondary analysis from being misrepresented as a new meteorological measurement campaign.

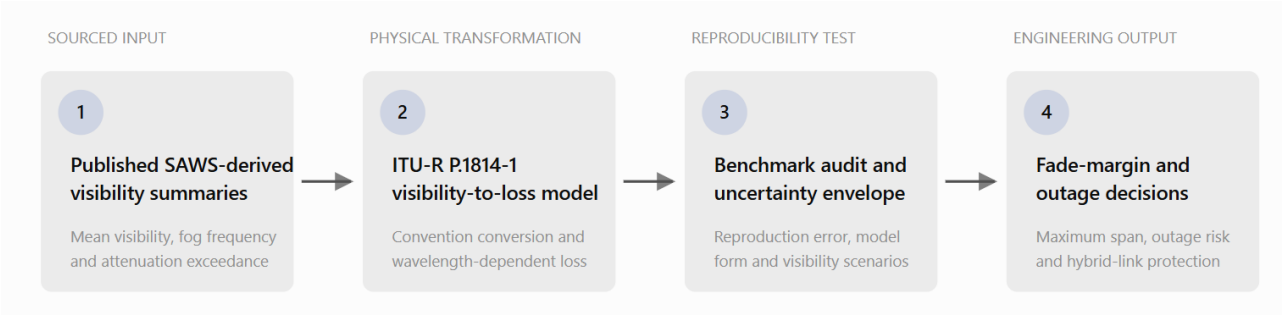


Fig. 1 Reproducible modelling and decision workflow

Figure 1 illustrates the reproducible workflow used to translate published SAWS-derived visibility statistics into practical FSO link-design decisions. The process begins with mean visibility, fog-frequency and attenuation-exceedance data, which are transformed into wavelength-dependent propagation losses using the ITU-R P.1814-1 model. The calculated losses are then subjected to benchmark reproduction, model-form assessment and visibility-uncertainty analysis to evaluate the reliability and sensitivity of the predictions. Finally, the validated outputs inform fade-margin allocation, maximum link-distance selection, outage-risk estimation and hybrid FSO/RF protection decisions. This structured separation between published inputs and newly derived results ensures methodological transparency, traceability and reproducibility.

3 Mathematical model

3.1 Optical power and atmospheric loss

For transmitted optical power P_t, system efficiency η_sys, geometric coupling G_geo(L), path length L and extinction coefficient σ_ext, mean received power is

$$P_r(\lambda,L,V) = P_t\, \eta_{sys}\, G_{geo}(L) \exp[-\sigma_{ext}(\lambda,V)L] \quad (1)$$

The specific attenuation and the corresponding homogeneous-path loss are

$$\gamma(\lambda,V) = 10 \log_{10}(e)\, \sigma_{ext}(\lambda,V) = 4.343\, \sigma_{ext}(\lambda,V) \quad (2)$$

$$A_{sp}(\lambda,V,L) = \gamma(\lambda,V)L \quad (3)$$

Equation (3) follows the homogeneous-fog approximation in ITU-R P.1814-1 and is applicable to terrestrial paths up to 5 km. The assumption is conservative when a local fog bank covers only part of the path and optimistic when spatially correlated dense fog extends beyond the point sensor.

3.2 Visibility convention and wavelength dependence

Meteorological optical range V is the path that reduces irradiance to 5% at approximately 550 nm. ITU-R P.1814-1 converts a 5% measurement to the 2% visibility convention used by the wavelength model, according to

$$V_2 = [\ln(0.02)/\ln(0.05)]V_5 = 1.306V_5 \quad (4)$$

For 0.4 μm ≤ λ ≤ 1.55 μm, the recommended specific attenuation is

$$\gamma_{sp}(\lambda,V_2) = (17/V_2)(0.55/\lambda)^{q(V_2)} \ \text{dB km}^{-1} \quad (5)$$

where λ is in micrometres and the exponent is

$$q(V) = \{1.6,\ V>50;\ 1.3,\ 6<V\leq 50;\ 0.16V+0.34,\ 1\leq V\leq 6;\ V-0.5,\ 0.5\leq V<1;\ 0,\ V<0.5\} \quad (6)$$

The 17/V constant corresponds to the 2% convention. If the meteorological station already reports 5% MOR, Eq. (4) must precede Eq. (5). Alternatively, a 5%-consistent 550 nm coefficient is $13/V_5$. Mixing 13, 17, V_5 and V_2 without conversion creates a deterministic bias of approximately 31%.

3.3 Probabilistic outage mapping

Let M_atm denote the atmospheric fade margin remaining after geometric, pointing, receiver and implementation losses. Conditional on a visibility realization, the fog-outage indicator is

$$I_{out}(V;\lambda,L,M_{atm}) = 1\{\gamma_{sp}(\lambda,V)L > M_{atm}\} \quad (7)$$

The corresponding outage probability is the visibility cumulative distribution evaluated at the critical visibility V_c:

$$P_{out} = P[A_{sp}>M_{atm}] = F_V(V_c) \quad (8)$$

$$V_c = \sup\{V>0 : \gamma_{sp}(\lambda,V)L > M_{atm}\} \quad (9)$$

Because q depends on V, Eq. (9) is solved piecewise or numerically. For a fixed q, an explicit inverse is available:

$$V_c(q) = (17L/M_{atm})(0.55/\lambda)^q \quad (10)$$

If fog occurrence is separated from conditional severity, with π_f=P(V<1 km), the hurdle representation is

$$P_{out} = \pi_f P[A_{sp}>M_{atm} \mid V<1] + (1-\pi_f)P[A_{sp}>M_{atm} \mid V\geq 1] \quad (11)$$

This identity is useful because it prevents frequent benign conditions from masking the rare fog tail. It does not impose a parametric form on either conditional distribution.

3.4 Link budget and maximum span

In decibels, the received-power budget may be written

$$P_{r,dBm} = P_{t,dBm} + G_{sys} - A_{geo}(L) - A_{point} - A_{sp}(\lambda,V,L) - A_{misc} \quad (12)$$

The atmospheric margin is therefore

$$M_{atm}(L) = P_{t,dBm} + G_{sys} - A_{geo}(L) - A_{point} - A_{misc} - P_{sens,dBm} \quad (13)$$

For a specified visibility and atmospheric margin, the maximum homogeneous-fog span is

$$L_{max}(V,\lambda,M_{atm}) = M_{atm} / \gamma_{sp}(\lambda,V) \quad (14)$$

3.5 Uncertainty propagation

A first-order relative sensitivity follows directly from Eq. (5). Within a region where q is constant,

$$\partial\ln\gamma/\partial\ln V = -1, \quad \partial\ln\gamma/\partial\ln\lambda = -q \quad (15)$$

Where q varies with visibility, the total visibility elasticity is

$$S_V = \partial\ln\gamma/\partial\ln V = -1 + V(dq/dV)\ln(0.55/\lambda) \quad (16)$$

For independent small uncertainties in V, L and q, a transparent variance approximation is

$$u^2(A_{sp})/A_{sp}^2 \approx u^2(L)/L^2 + S_V^2u^2(V)/V^2 + [\ln(0.55/\lambda)]^2u^2(q) \quad (17)$$

For finite visibility error ε, non-linear bounds avoid the small-error assumption:

$$A^- = L \min_{v\in[V(1-\varepsilon),V(1+\varepsilon)]}\gamma(\lambda,v), \quad A^+ = L \max_{v\in[V(1-\varepsilon),V(1+\varepsilon)]}\gamma(\lambda,v) \quad (18)$$

These are scenario envelopes, not confidence intervals, because the measurement-error distribution is unavailable.

4 Numerical experiments and validation strategy

4.1 Benchmark reproduction audit

Table 2 reproduces the published South African mean-visibility benchmark. Direct inspection showed that the reported wavelength values are too small to be specific attenuation from Eq. (5), but they are nearly exact for a 0.23 km path with q=1.3 and the 2% constant. The audit therefore tests A=0.23γ rather than relabelling the values as dB/km.

Table 2 Published SAWS-derived values and effective path length inferred using q=1.3

Location	V (km)	650 nm	850 nm	1550 nm	Back-calculated L (km)
Cape Town	18.370	0.171	0.121	0.055	0.2295
Bloemfontein	7.400	0.425	0.300	0.137	0.2297
Pretoria	24.930	0.126	0.089	0.041	0.2302
Emalahleni	4.400	0.715	0.505	0.231	0.2300
East London	4.800	0.656	0.463	0.212	0.2302
Polokwane	8.700	0.362	0.255	0.117	0.2301
Upington	9.870	0.319	0.225	0.103	0.2300

Across all 21 location-wavelength pairs, the recomputation gives MAE=0.000216 dB, RMSE=0.000252 dB, MAPE=0.133%, and R^2=0.999998. The effective path length has mean 0.22997 km and sample standard deviation 0.00049 km. Figure 2 confirms that the correspondence is not driven by one wavelength or location.

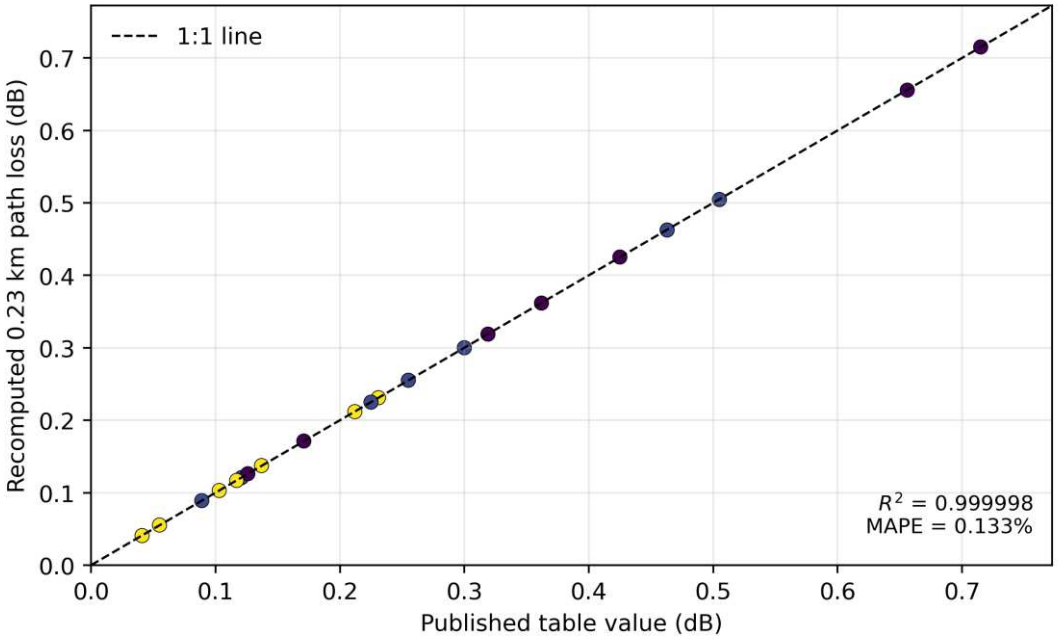


Fig. 2 Numerical reproduction of the published seven-location benchmark using A = 0.23γ and q = 1.3

This is implementation verification, not an independent atmospheric validation, because the benchmark values appear to have been generated from the same visibility equation. The near-perfect agreement should therefore be interpreted as evidence that the equations were implemented correctly, rather than as confirmation that the visibility model is unbiased under South African fog conditions.

4.2 Model-form sensitivity

Figure 3 compares the current ITU piecewise exponent with the fixed q=1.3 convention implicit in the benchmark. In the haze regime above 6 km the two coincide. Between 1 and 6 km the piecewise

exponent decreases with visibility. Below 0.5 km, ITU sets q=0, so the predicted fog attenuation becomes wavelength independent. Thus the strong 1550 nm advantage present in mean-visibility tables should not be extrapolated into dense-fog conditions.

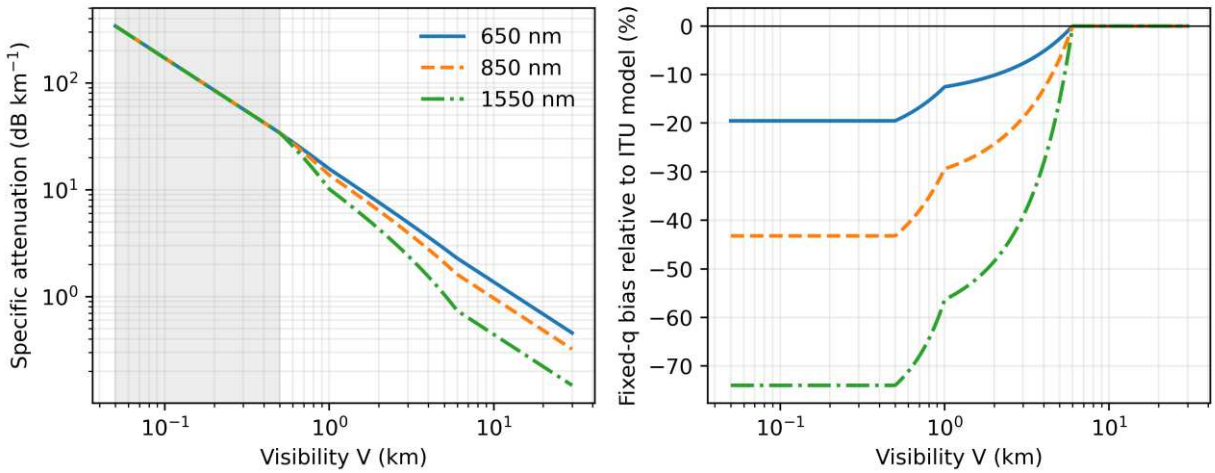


Fig. 3 ITU-R P.1814-1 attenuation and structural bias caused by retaining q = 1.3 outside its validity interval

4.3 Visibility-error scenarios

Table 3 applies Eq. (18) to a 230 m, 1550 nm path at the seven mean visibilities. The ±10% and ±20% columns are deterministic perturbations of reported visibility, useful when sensor uncertainty and microclimate representativeness cannot be separated. Because attenuation is approximately inversely proportional to visibility in this regime, a 20% visibility perturbation reduces loss by roughly 25%.

Table 3 Deterministic visibility uncertainty envelopes for a 0.23 km, 1550 nm path

Location	Nominal loss (dB)	±10% V envelope (dB)	±20% V envelope (dB)
Cape Town	0.055	0.050-0.061	0.046-0.069
Bloemfontein	0.137	0.125-0.153	0.114-0.172
Pretoria	0.041	0.037-0.045	0.034-0.051
Emalahleni	0.231	0.210-0.257	0.193-0.289
East London	0.212	0.193-0.235	0.177-0.265
Polokwane	0.117	0.106-0.130	0.097-0.146
Upington	0.103	0.094-0.114	0.086-0.129

4.4 Margin-to-distance design boundaries

Figure 4 evaluates Eq. (14) at 1550 nm. At V=0.1 km, q=0 and γ=170 dB km^{-1}, so margins of 20, 40 and 60 dB support only 0.118, 0.235 and 0.353 km, respectively. At V=0.5 km, q=0 and γ=34 dB km^{-1}, so the same margins support 0.588, 1.176 and 1.765 km. The result quantifies why path shortening is the most reliable means of mitigating dense fog.

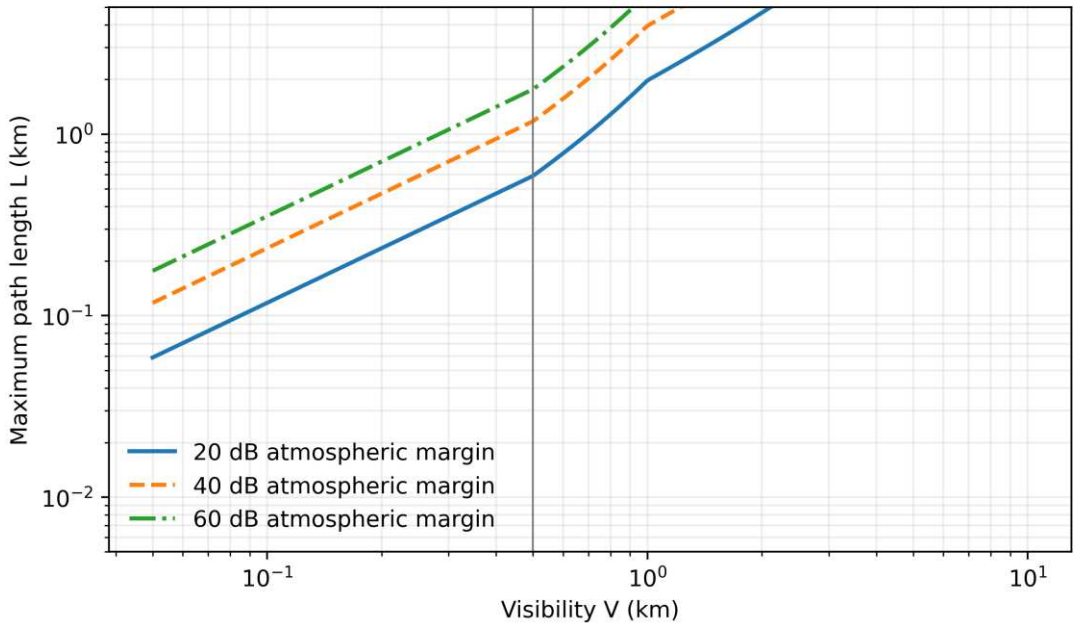


Fig. 4 Maximum 1550 nm homogeneous-fog path length as a function of visibility and atmospheric margin

4.5 Published severe-loss exposure

Kolawole et al. (2022) report selected probabilities that attenuation exceeds 80 dB km^{-1}. If these sample probabilities are treated as stationary climatological frequencies, then annual exposure is h = 8760p. This conversion yields an interpretable engineering quantity but not an event-duration distribution.

Table 4 Derived annual exposure from published attenuation exceedance probabilities

Location	P(γ>80 dB km^{-1})	Annualized exposure (h year^{-1})	99.9% budget exceeded?
Mbombela	0.0038	33.3	Yes
Cape Town	0.0026	22.8	Yes
Polokwane	0.0012	10.5	Yes

The severe-loss exposure alone exceeds the 8.76 h annual unavailability allowance associated with 99.9% availability at all three sites. This comparison is conservative only with respect to the 80 dB km^{-1} threshold: actual outage depends on the span and fade margin, while equipment, pointing, and power failures introduce additional mechanisms of unavailability.

5 Discussion

5.1 What the validation establishes

The audit establishes traceability. A reader can reproduce the South African table using the stated visibility equation, wavelength exponent, and a 230 m path. It also corrects a consequential unit ambiguity: the numerical values correspond to path attenuation, whereas a dB/km interpretation understates specific attenuation by a factor of about 1/0.23 = 4.35. This distinction affects every link budget built from the table.

The agreement is not a meteorological validation. Both the benchmark and the recomputation are deterministic transformations of mean visibility. Proper empirical validation requires time-matched optical attenuation or received-power measurements, station visibility, weather codes, quality flags and a predeclared hold-out period. The present model should therefore be used for screening and transparent scenario analysis, not as a certified site-availability guarantee.

5.2 Why the probabilistic tail dominates

Mean visibility describes routine operation, but not rarely dense fog. In the ITU model, the wavelength exponent approaches zero below 0.5 km; 650, 850 and 1550 nm then share the same visibility-derived scattering loss. Consequently, selecting 1550 nm improves mean-weather performance and eye-safety power headroom, but does not eliminate catastrophic fog outages. Diversity or a shorter span is required when availability targets are stricter than the local fog-tail probability.

5.3 South African deployment implications

For Mbombela and Cape Town, the published severe-tail exposure is already incompatible with a standalone 99.9% target if the deployed link tolerance is exceeded by 80 dB km ^{1}. Polokwane is also above that availability budget. A defensible architecture should therefore combine conservative span selection with received-power or visibility-triggered switching to radio frequency, spatially diverse routes, or both. Switching thresholds should be calculated from Eq. (9) for the actual equipment margin and should include hysteresis to prevent rapid state changes near the boundary.

Airport or station visibility may not reflect the optical-path microclimate. ITU-R P.1814-1 explicitly warns that visibility is microclimate-sensitive. A rooftop path near cooling towers, wetlands, or a valley can differ from that of a nearby synoptic station. Site acceptance should therefore pair a transmissometer or calibrated visibility sensor with logged received optical power along the intended path.

5.4 Comparison with related FSO work

The formulation is consistent with laboratory evidence that visibility-based models diverge in dense fog (Ijaz et al. 2013) and with South African feasibility studies emphasizing location-dependent conditions (Mohale et al. 2016; Kolawole et al. 2022; Maswikaneng et al. 2022). Recent South African machine-learning work uses broader meteorological predictors, but predictive accuracy does not eliminate the need to specify measurement convention, path length, and temporal split. The present contribution is complementary: it supplies an auditable physical baseline against which more flexible models can be tested.

6 Recommended station-level validation protocol

A future raw-data extension should be preregistered before fitting. At minimum, acquire timestamped SAWS MOR, present-weather codes, temperature, relative humidity, wind and rainfall, together with synchronized received power from a calibrated 850 or 1550 nm path. Convert visibility conventions once, retain quality flags, and avoid averaging across fog and non-fog states.

Table 5 Minimum protocol for a defensible raw SAWS and field-link validation study

Stage	Required action	Primary diagnostic
Ingestion	Preserve timestamps, station identifiers, sensor limits and weather codes	Missingness and censoring map
Alignment	Synchronize MOR and received power; document averaging interval	Lag sensitivity
Calibration	Estimate only justified parameters on earlier years	Residual bias by visibility bin
Temporal validation	Hold out the latest complete year or fog season	MAE, RMSE and calibration of exceedance
Spatial validation	Leave one station or path out	Transfer error and uncertainty width
Tail validation	Use block bootstrap by fog event, not independent rows	Coverage of 99th and 99.9th percentiles
Decision validation	Test margin-derived outage alarms	Precision, recall and outage-hours error

For observations y_i and predictions $\hat{y}_i$, report MAE and RMSE, but also test exceedance calibration because outage is the target quantity:

$$\mathrm{MAE} = n^{-1}\Sigma|y_i\text{-}\hat{y}_i|, \qquad \mathrm{RMSE} = [n^{-1}\Sigma(y_i\text{-}\hat{y}_i)^2]^{1/2} \tag{19}$$

$$\mathrm{Brier}(\tau) = n^{-1}\Sigma[1\{y_i>\tau\}\text{-}\hat{p}_i(\tau)]^2 \tag{20}$$

Confidence intervals should be estimated from complete fog events or days to preserve temporal dependence. A random row split would leak autocorrelation and exaggerate performance.

7 Limitations

The analysis is constrained by published aggregates. It cannot reconstruct event duration, seasonality, serial dependence, censoring at sensor limits, visibility measurement uncertainty or joint rain-fog occurrence. Annualized hours assume that published sample frequencies are stationary and representative. The homogeneous-path approximation ignores fog patchiness. The seven-location numerical audit verifies the implementation, but it is not independent, as the published values were evidently generated by the same model family. No claims are made about bit-error rate without specifying modulation, receiver bandwidth, detector noise and turbulence. These limitations define the boundary of the conclusions rather than invalidate the screening framework.

8 Conclusion

A scientifically rigorous South African FSO model must clearly distinguish between measured data, derived results and aspects that remain empirically unvalidated. This study aligns the attenuation equations with ITU-R P.1814-1, derives outage and uncertainty relations, and numerically reproduces a published SAWS-derived benchmark. The reproduction identifies a 0.23 km implicit path length and prevents path loss from being mistaken for dB/km specific attenuation. The analysis further shows that the 1550 nm advantage diminishes in dense fog under the current ITU exponent, so link shortening and protected hybrid operation are more reliable than wavelength choice alone. Assuming that a specific attenuation threshold of \(80\ \text{dB km}^{-1}\) causes link outage, the published exceedance probabilities correspond to annual severe-attenuation exposure durations greater than the \(8.76\)-hour unavailability allowance associated with a 99.9% annual availability target in Mbombela, Cape Town, and Polokwane. The proposed framework supports preliminary FSO link planning and provides a structured basis for subsequent station-level validation; however, operational validation requires original, temporally aligned SAWS observations and corresponding optical-link measurements.

References

Adebusola, S.O., Owolawi, P.A., Ojo, J.S., Maswikaneng, P.S., Ayo, A.O.: Application of principal component analysis and artificial neural networks for the prediction of QoS in FSO links over South Africa. Results in Optics (2025).

Alatawi, A.S., Youssef, A.A., Abaza, M., Uddin, M.A., Mansour, A.: Effects of atmospheric turbulence on optical wireless communication in NEOM smart city. Photonics 9, 262 (2022). https://doi.org/10.3390/photonics9040262

Alimi, I.A. and Monteiro, P.P.: Revolutionizing free-space optics: A survey of enabling technologies, challenges, trends, and prospects of beyond 5G free-space optical (FSO) communication systems. Sensors, 24(24), p.8036. (2024)

EL-Qady, A., Abaza, M.: Performance analysis of the effects of atmospheric turbulence on free space optical communication using multi-hop decode and forward relay in north and south of Egypt. Opt. Quantum Electron. 56, 1373 (2024). https://doi.org/10.1007/s11082-024-07259-w

arimo, C.P., Rashidi, F.U. and Kaijage, S.F. (2026) 'Evaluating the impact of fog on free space optical communication links in Mbeya and Morogoro, Tanzania', Photonics, 13(2), Article 110. https://doi.org/10.3390/photonics13020110

International Telecommunication Union: Prediction methods required for the design of terrestrial free-space optical links. Recommendation ITU-R P.1814-1, Geneva (2025).

Khan, M.S., Awan, M.S., Faisal, M., Muhammad, S.S., Mathiopoulos, P.T.: Probabilistic model for free-space optical links under continental fog conditions. Radioengineering 19, 460-465 (2010).

Kolawole, O.O., Afullo, T.J.O., Mosalaosi, M.: Terrestrial free space optical communication systems availability based on meteorological visibility data for South Africa. SAIEE Afr. Res. J. 113, 20-36 (2022). https://doi.org/10.23919/SAIEE.2022.9695423

Maswikaneng, P.S.: Atmospheric attenuation impact on free-space optical propagation paths: a case of South Africa. Adv. Space Res. 72, 3856-3868 (2023).

Maswikaneng, P.S., Owolawi, P.A., Afullo, T.J.O.: Estimating effect of total specific atmospheric attenuation on the performance of free space optical communication link: a South African case. J. Commun. 17, 498-509 (2022). https://doi.org/10.12720/jcm.17.7.498-509

Mohale, J., Handura, M.R., Olwal, T.O., Nyirenda, C.N.: Feasibility study of free-space optical communication for South Africa. Opt. Eng. 55, 056108 (2016). https://doi.org/10.1117/1.OE.55.5.056108

Nadeem, F., et al.: Continental fog attenuation empirical relationship from measured visibility data. Radioengineering 19, 596-600 (2010).

Singh, H., Miglani, R., Mittal, N., Gaba, G.S., Masud, M., Aljahdali, S.: Design and analysis of commercially viable free-space optical communication link for diverse beam divergence profiles. Front. Phys. 9, 778734 (2021). https://doi.org/10.3389/fphy.2021.778734

Yasir, S.M., Abas, N., Rahman, A., Saleem, M.S.: Simulation analysis of adaptive FSO/RF hybrid link under diverse weather conditions of Lahore, Pakistan. Results Opt. 2, 100047 (2021). https://doi.org/10.1016/j.rio.2020.100047

Statements and Declarations

Funding: The author declares that no funds, grants, or other support were received during the preparation of this manuscript.

Competing interests: The author declares no competing financial or non-financial interests.

Author contributions: Phatle Solly Maswikaneng- conceptualization, methodology, numerical analysis, visualization, writing and revision. The author accepts responsibility for the integrity of the work.

Data availability: This secondary analysis uses numerical summaries published by Kolawole et al. (2022) and Maswikaneng et al. (2022). The underlying station-level SAWS observations were not available to the author and are not redistributed. All equations, benchmark values and derived calculations needed to reproduce the results are reported in the manuscript. Access to original SAWS records remains subject to the data provider and the cited studies.

Code availability: The calculations use the explicit equations and tabulated inputs reported in this article. A machine-readable implementation should be deposited in a public repository before submission, and its persistent identifier should be inserted here: [repository DOI].

Ethics approval: Not applicable. The study uses published meteorological summaries and contains no human participants or animals.

Consent to participate: Not applicable.

Consent for publication: Not applicable.

Use of generative artificial intelligence. Generative artificial intelligence was used to assist with manuscript drafting, numerical scripting and language refinement. The author must verify all equations, calculations, citations and interpretations, assumes full responsibility for the final manuscript, and should revise this statement to match the actual workflow before submission.